Journal of Chemical Health Risks

www.jchr.org

JCHR (2024) 14(6), 2129-2143 | ISSN:2251-6727

In-vitro and In-vivo Characterization of Melatonin-Loaded Nanoparticles for the Treatment of Inflammatory Bowel Disease

Kamdev Sen[1], Priya Patel[2], Pradeep Kumar Samal[1], Khileshwari*[3], Shashank Kumar Tiwari[4], Aditi Bhatt[5], Neha Baghel[6], Jhakeshwar Prasad[7]

[1]Guru Ghasidas Vishvavidyalay, Koni Bilaspur - 495009, Chhattisgarh, India

[2]Rungta Institute of Pharmaceutical Science and Research, Kohka, Kurud – 490024, Bhilai, Chhattisgarh, India

[3]Rungta College of Pharmaceutical Sciences and Research, Kohka, Kurud – 490024, Bhilai, Chhattisgarh, India

[4]Lords International College of Pharmacy Alwar-Bhiwadi Rd, Chikani – 301028, Rajasthan, India

[5]Metro College of Health Sciences and Research, Greater Noida - 201310, Uttar Pradesh, India

[6]Shyam Balaji Pharmacy College, Mahasamund - 493445, Chhattisgarh, India

[7]Shri Shankaracharya College of Pharmaceutical Sciences, Junwani – 490020, Bhilai, Chhattisgarh, India

***Corresponding Author -** Khileshwari; Rungta College of Pharmaceutical Sciences and Research, Kohka, Kurud, Bhilai, Chhattisgarh, India

Email id. - nishadkhileshwari75@gmail.com

(Received: 16 September 2024 Revised: 11 October 2024 Accepted: 11 December 2024)

KEYWORDS
Melatonin; Inflammatory bowel disease; Ulcerative colitis; Pharmacological treatment

ABSTRACT:

Inflammatory Bowel Disease (IBD) is a complex inflammatory condition arising due to interactions of environmental and genetic factors that lead to dysregulated immune response and inflammation in intestine. Complementary and alternative medicine approaches have been utilized to treat IBD. However, chronic inflammatory diseases are not medically curable. Hence, potent anti-inflammatory therapeutic agents are urgently warranted. Melatonin has emerged as a potent anti-inflammatory and neuroprotective candidate. Although, it's therapeutic efficacy is compromised due to less solubility and rapid clearance. Hence, we have synthesized melatonin loaded chitosan nanoparticle to improve drug release profile and evaluate its *in-vitro* and *in-vivo* therapeutic efficacy. Mel-CSNPs exhibited better anti-inflammatory response in an *in-vitro* and *in-vivo* IBD model. Significant anti-inflammatory activity of Mel-CSNPs is attributed to nitric oxide (NO) reduction, inhibited nuclear translocation of NF-kB p65 and reduced IL-1β and IL-6 expression. *In-vivo* biodistribution study has shown a good distribution profile. Effective *in-vivo* therapeutic efficiency of Mel-CSNPs has been confirmed with reduced disease activity index parameters and inhibited neutrophilic infiltration. Histological evaluation has further proved the protective effect of Mel-CSNPs by preventing crypt damage and immune cells infiltration against Dextran Sodium Sulphate induced insults. Immuno-histochemical analysis has confirmed anti-inflammatory action of Mel-CSNPs with reduction of inflammatory markers, Nitric Oxide Synthase-2 and Nitrotyrosine. Indeed, this study divulges anti-inflammatory activity of Mel-CSNPs by improving the therapeutic potential of melatonin.

1. Introduction

Inflammatory Bowel disease (IBD) is an idiopathic condition resulting from dysregulated immune response to the host gut microbiota. There are two major pathological conditions included in this category

which includes Ulcerative Colitis (UC) and Crohn's Disease (CD). Ulcerative Colitis (UC) includes condition in which there is ulceration in mucosal and submucosal region of colonic tissue leading to gutepithelial layer damage which is limited to colon and rectum region of gastrointestinal tract [1]. Histological finding of UC is characterised by acute and chronic inflammation of polymorphonuclear leukocytes, mononuclear cells, pus, crypt damage and goblet cells depletion [2]. Crohn's Disease (CD) can occur in any

Journal of Chemical Health Risks

www.jchr.org

JCHR (2024) 14(6), 2129-2143 | ISSN:2251-6727

region of gastrointestinal tract but it is most commonly observed in ileocecal region. In that, inflammation can extend up to serosa resulting into sinus tracts. Histological examination may reveal inflammation extending to the submucosal region and may be accompanied by non-caseating granuloma formation [3]. Rectal bleeding occurs more often in UC patients whereas patients suffering from CD shows weight loss and perianal disease. Indeed, risk of autoimmune disease is higher in person suffering from CD compared to normal individual [4]. The prevalence of IBD is rising globally which raises the issue of developing colorectal cancer in the near future. As per a report, 3.9 million females and 3 million males of the globe are living with IBD. Earlier, it was believed that IBD is only prevalent in developed countries. However, the prevalence of IBD is also increasing in developing countries which raise the alarming condition about risk of this disease. Pharmacological intervention used for treatment of IBD at present include salicylates, immuno-modulators, corticosteroids, and anti-TNFalpha agents [5]. In spite of limited therapeutic efficacy, these agents show undesirable toxic effects which limits their application as curative agent. Immunotherapy is also available for IBD treatment but the cost of immunotherapy compromises its application and viability to common individuals [6, 7]. Hence, new pharmacological agents having better therapeutic effects are warranted for IBD treatment. Melatonin is naturally occurring neuro-hormone which has higher therapeutic potential with anti-inflammatory, antioxidant and neuroprotective activity [8]. Melatonin is available over the counter (OTC) which suggests its safety parameter. Melatonin has shown a promising potential as anti-inflammatory agent in murine model Ulcerative colitis (UC) [9]. Apart from being highly potent drug, the therapeutic efficacy of melatonin is compromised due to its poor solubility and burst drug release which increases its dosing interval and therapeutic dose also [10]. Hence to overcome this limitation, we have synthesized chitosan based nano-formulation of melatonin to improve the therapeutic potential of melatonin. Chitosan being highly biodegradable, biocompatible and non-toxic is widely studied as a pharmaceutical excipient. Chitosan is a naturally occurring cationic polymer of glucosamine and N-acetyl-glucosamine having pKa of 6.5 which makes it soluble in acidic condition due to protonation of amine group [11]. In recent era, nanotherapeutic approaches based on nano-drug delivery system has gain attention. Chitosan nanoparticles based drug delivery system is also widely studied in improvement of drug release profile and therapeutic efficacy of hydrophobic drug molecules [12]. Hence, we encapsulated melatonin in chitosan nanoparticles to enhance its therapeutic efficacy by improving melatonin release profile. Here, we have synthesized melatonin loaded chitosan nanoparticle following ionic gelation method using anionic sodium tripolyphosphate to explore it's in-vitro and in-vivo therapeutic potential [13]. Invitro therapeutic efficacy is evaluated against LPS stimulated macrophages model and DSS-induced Ulcerative colitis mouse model is followed to analyse in-vivo therapeutic potential. Here, we first demonstrated therapeutic efficiency of melatonin loaded chitosan nanoformulation in IBD treatment [14].

2. Materials and methods

Low molecular weight chitosan (5–20 mPa), melatonin and o-dianisidine hydrochloride were purchased from TCI Chemicals Mumbai, India. Sodium tripolyphosphate (STPP) and lipopolysaccharide (LPS) were purchased from Sigma-Aldrich Mumbai, India. Primary antibodies NFkB p65 and Nitric Oxide Synthase (NOS2) were purchased from SCBT and Nitro-tyrosine was purchased from Sigma-Aldrich, Mumbai, India. Secondary Fluorescein Isothiocyanate (FITC) conjugated anti-rabbit IgG and Tetramethylrhodamine Isothiocyanate (TRITC) conjugated anti-mouse IgG were purchased from SCBT. Haematoxylin and Eosin were purchased from Himedia lab. Alcian Blue and Nuclear Fast Red were purchased from Mumbai, India. All the reagents used in synthesis were of analytical grade with ≥98% purity.

Preparation of chitosan nanoparticles (CSNPs) and melatonin loaded chitosan nanoparticles

Polymeric nanoparticles of chitosan were prepared using ionic gelation method, with some modifications [15]. For preparation of CSNPs, 6 mg of low molecular weight chitosan was dissolved in 4 mL of 1% aqueous acetic acid (1.5 mg/mL). STPP solution was dissolved in Type-1 water (3 mg/mL) and added gradually dropwise through 1 mL syringe under continuous magnetic stirring (360 rpm) condition till opalescent

Journal of Chemical Health Risks

www.jchr.org

JCHR (2024) 14(6), 2129-2143 | ISSN:2251-6727

dispersion is achieved which indicates formation of nanoparticles [16]. CSNPs were centrifuged at 15000 rpm, washed 3 times for purification and lyophilised for future application. The ratio of Chitosan and STPP was optimised to be 2:1 for nanoparticle synthesis. For preparation of melatonin loaded chitosan nanoparticles (Mel-CSNPs), different weight/weight ratio of melatonin with respect to polymer were used. Melatonin was added into the chitosan solution and allowed to interact for 1 h, then nanoparticles were formed by cross linking using STPP through ionic gelation method and methanol was evaporated to enhance entrapment of drug into the nanoparticles [17]. Drug and polymer ratio was considered as 1:10, 1:5 and 1:2 for nanoformulation optimization. For characterisation study of drug loaded nanoparticles we have used only 1:2 ratio. For preparation of Fluorescein Isothiocyanate (FITC) labelled chitosan nanoparticles, chitosan (100 mg) was dissolved in 1% acetic acid and 1 mg of FITC was allowed to react for 12 h. The reacted chitosan and FITC was then dialysed against deionised water for 72 h for removal of unreacted part. This fluorescent conjugated chitosan was then used to prepare FITC-CSNPs using ionotropic gelation method using STPP or lyophilized for future applications [18].

Fourier transforms infrared (FTIR) and X-ray diffraction (XRD) analysis

FTIR analysis of chitosan, melatonin, CSNPs and Mel-CSNPs were performed for functional group characterisation. Briefly, 2 mg of powdered sample were mixed potassium bromide (KBr) and pellet was formed using hydraulic pressure. The pellets were scanned for analysis and spectra were recorded 4000-400 cm- 1 for each sample. The changes in crystallinity of melatonin was evaluated using X-ray diffraction (XRD) analysis after formation of nanoparticles and compared with chitosan and chitosan nanoparticles.

***In-vitro* drug release study**

In-vitro drug release of Mel-CSNPs was performed using dialysis bag method. Briefly, 5 mg melatonin loaded CSNPs was filled in dialysis bag and placed in sink condition, 0.1% tween 20 containing PBS pH 7.4 and acetate buffer pH 4.5.The system was stirred at 30 rpm and 1 mL of samples was taken at predefined time intervals (0, 0.5, 1, 3, 6, 12 and 24 h) refilled with fresh buffer of equal volume to maintain sink condition. The samples were analysed using multimode plate reader (Tecan Inc.) at 278 nm for evaluating the drug release profile of Mel-CSNPs [19].

***In-vitro* cellular uptake study**

In-vitro cellular uptake study was performed for FITC-tagged CSNP to determine the uptake of nanoparticles in RAW 264.7 murine macrophages procured from National Centre of Cell Science (NCCS), Pune. The cells were maintained in Dulbecco Minimum Essential Medium supplemented with 10% heat inactivated fetal bovine serum (FBS) (Gibco), 100UmL- 1penicillin and 100 µgmL- 1 streptomycin. Cell line was maintained at 37 ◦C and 5% CO2 in humidified incubator. Cells were harvested and 5x105cells were seeded on sterile poly-L-lysine coated coverslips. Briefly, cells were treated with FITCtagged nanoparticles for 1 h and thereafter, coverslips were washed with chilled 10 mM phosphate buffer saline (PBS) pH 7.4 and fixed with 4% paraformaldehyde solution. Nucleus of the cells was counter stained using DAPI (4′, 6-diamidino-2-phenylindole) before mounting on a glass slide. These cells were observed in a confocal laser scanning microscope to analyse the cellular localisation of FITC-tagged chitosan nanoparticles.

Nitrite estimation (NO)

To estimate anti-inflammatory potential of nanoformulation in-vitro model of inflammation induced using LPS (1 µg/mL) was followed. Cells were pre-treated with nanoparticles for 1 h then treated with LPS for 24 h. The nitrite estimation was performed using Griess method for NO detection. Briefly, 100 µL of cell supernatant is mixed with 100 µL of Griess Reagent, incubated at room temperature 10 min in the dark. The absorbance was recorded at 540 nm [20].

Haemolysis assay

The blood was collected in 3.8% sodium citrate was centrifuged to collect Red Blood Cell (RBC) for haemolysis test of the nanoparticles by following methodology of our previous study [21]. Briefly, 10 time

dilution of 1 mL of RBC was prepared using PBS pH 7.4. 900 µL of diluted RBC was added to 100 µL nanoparticles and melatonin loaded suspensions. 0.1% Triton-X 100 and saline were used as positive and

Journal of Chemical Health Risks

www.jchr.org

JCHR (2024) 14(6), 2129-2143 | ISSN:2251-6727

negative control, respectively. Finally, 2 mL micro centrifuge tubes were incubated at 37 ◦C and centrifuged at 3500 rpm for 10 min [22]. The collected supernatant was utilized to estimate OD values at 540 nm to determine the % haemolysis using the following equations.

Haemolysis % = (OD of the samples – OD of the negative control)/ (OD of the positive control – OD of the negative control).

Animals

All the animal experiments were approved by the Institutional animal ethical committee (IAEC) with approved animal study protocol number IAEC 17/29 and performed as per guidelines provided by the Committee for the Purpose of Control and Supervision of Experiments on Animals (CPCSEA). Appropriate measures were taken to reduce the pain or any discomfort to experimental animals during study and final sacrifice. Balb/C mice of 6–8 weeks were housed in a 12 h light/dark cycle under controlled environmental conditions at standard 25 ± 2 ◦C with 50 ± 10% humidity. Animals were provided standard chow diet and drinking water.

***In-vivo* biodistribution study**

Animals were acclimated for three days prior commencement of the experimental study. The fur of the mouse was removed from the thoracic and abdominal region using hair remover cream. Indocyanine green (ICG) tagged Mel-CSNP (4 mg/mL) was dispersed in sterile saline solution and administered intravenously. Indocyanine green is a fluorescent dye generally used as a medical diagnostics agent used for evaluating cardiac output, hepatic function, liver and gastric blood flow which makes it a highly suitable agent for determining bio-distribution of MelCSNPs. ICG has spectral absorbance at about 800 nm. The imaging was performed using a whole body imaging system for animals at different time points for bio-distribution analysis of ICGtagged Mel-CSNPs. At the end of the experiment, mice were sacrificed using CO2 asphyxiation method and vital organs were collected and imaged using IVIS for tissue distribution study analysis.

Development of animal model and efficacy studies

Female Balb/C mice were randomly divided in 5 groups (n = 6). DSS (36–50 k Da) was given at 5% w/v in drinking water for five days for induction of ulcerative colitis. For developing Dextran Sodium Sulphate (DSS) induced Inflammatory Bowel Disease (Ulcerative Colitis) in mouse model, DSS (36–50 k Da) was administered orally by dissolving in autoclaved drinking water (5% w/v) for 5 days. Treatment with drug and nanformulations were given simultaneously for their anti-inflammatory in-vivo efficacy study. The animals were divided in 5 groups: group 1- Control, group 2- DSS, group 3- DSS + CSNPs, and group 4- DSS + Melatonin and group 5-DSS + Mel-CSNPs.

Disease activity index (DAI), % bodyweight and colon length

Disease activity index was calculated to assess the severity based on following parameters like stool blood, stool consistency, and loss in body weight. Scoring was done based on parameters shown in Table S1. Degree of inflammation is also determined by change in colon length. Shortening of colon indicates severity of inflammation induced in mouse by DSS treatment. In order to assess the anti-inflammatory activity of melatonin and Mel-CSNPs, we have measured the colon length after sacrificing each mouse [23].

Myeloperoxidase (MPO) assay

Tissue samples of colon from mice were collected, cleaned with forceps to remove faecal matter, weighed and placed in 1.5 mL sterile Eppendorf microcentrifuge tubes. Tissue samples were placed on ice all time during this process. Tissues were homogenised using hand homogeniser in appropriate amounts of hexadecyltrimethylammonium bromide (HTAB) buffer according to their weight (50 mg/mL). After complete homogenisation of tissues, clear supernatants were collected by centrifuging for 6 min (13,400 x g, 4 ◦C). Supernatants were collected, were used for MPO assay and unused samples were stored in – 80 ◦C. For MPO assay, o-dianisidine solution (100 mL) prepared by mixing 16.7 mg o-dianisidine dihydrochloride in 90 mL of Type-1 water and 10 mL potassium phosphate buffer. The solution should be freshly prepared for every assay. 7 µL of tissue supernatants were placed in 96 well plates. 50 mL of 3% H2O2 was added to each well to o-dianisidine mixture. 200 µL H2O2 containing o-dianisidine was added to each well. Absorbance at 450

Journal of Chemical Health Risks

www.jchr.org

JCHR (2024) 14(6), 2129-2143 | ISSN:2251-6727

nm was recorded using spectrophotometer (Tecan Inc.). Triple readings were recorded at 30 s intervals. MPO activity was calculated to assess the therapeutic efficacy of nanoformulations [24].

Haematoxylin and eosin (H&E)

Histological study for evaluations of pathological alterations during DSS induced inflammatory conditions in colonic tissue sections were carried out using H&E staining. After sacrificing animals, colon tissue were collected and in formalin solution for 1 week. Briefly, the tissues were frozen in optimal cutting temperature media and sectioned in 7 µm thickness using Cryo-microtome. The sections were stained and microscopically examined for evaluation of pathological changes. The sections were mounted on poly-L-lysine coated slides and stained using standard staining protocol. Briefly, slides were washed in distilled water for 3 times (5 min) followed by 10 min staining in Haematoxylin solution. Followed by a single dip in ammonia water (bluing agent) and washed with DI water. After which the slides were stained with Eosin solution for 30 s, followed by dehydration using gradient alcohol method and finally dipped in xylene for complete dehydration. Finally slides were mounted using permanent mounting medium (DPX) and allowed to dry for 24 h These stained slides were observed and imaged using an optical microscope. For Histological scoring; H&E stained sections were scored blindly using the published system for the assessment disease severity. Crypt architecture, muscle thickness, degree of inflammatory cell infiltration (normal-0, dense inflammatory infiltrate- 3), goblet cell depletion (absent-0, present-1) and crypt abscess (absent- 0, present-1).

Alcian blue and nuclear fast red

Colonic tissue section slides were washed and hydrated with deionised water. The slides were placed in Alcian Blue staining solution for 30 min followed by washing in running tap water for 2 min [25]. The slides were rinsed with deionised water, counterstained using Nuclear Fast Red for 5 min and washed in running tap water for 1 min. Slides were dehydrated using alcohol gradients and cleared with xylene. Finally, it was mounted with a resinous mounting medium DPX. Alcian Blue stains goblets cells in blue colour whereas Nuclear Fast Red is used as counter stain for staining nuclei of epithelial cells. Loss of goblet cells observed per crypt can be used as parameter for assessing the intensity of disease [26].

Nitric oxide synthase (NOS2) and nitro-tyrosine

Immuno-histochemical study for expression of NOS2 and Nitrotyrosine which are prominent protein biomarkers for inflammatory condition. Briefly, colonic tissue was collected after animals were sacrificed and fixed using a 4% formalin solution in PBS pH 7.4. The fixed colonic tissues were treated with 10%, 20% and 30% sucrose solution prior cutting sections on Cryo-microtome. 7-10 µm sections were taken on poly-L-lysine coated glass slides by fixing then in Optimum Cutting Temperature (OCT) medium. The tissue sections were washed with PBS-Triton-X-100, 0.1% solution to remove OCT. Blocking was done using 5% Bovine Serum Albumin for 1 h. Primary NOS2 (1:250) and Nitro-tyrosine (1:250) antibody were treated on the tissue section at 4 ◦C for 24 h under humid condition. After treatment with primary antibody, secondary antibodies conjugated with fluorescent dye were used for imaging. The sections were observed and imaged using fluorescence confocal laser microscopy.

Statistical analysis

All data were calculated as ±SEM of each experiment, for in-vitro (n = 3) and in-vivo (n = 6). Significance was determined using analysis of variance (ANOVA) followed by Tukey's post-test using GraphPad Prism6. For significance (*$p \leq 0.05$, **$p \leq 0.001$ and ***$p \leq 0.0001$).

3. Results and discussion

Size and morphological analysis of nanoparticles

The mean hydrodynamic size of CSNPs and Mel-CSNPs were observed to be 135 nm and 155 nm through dynamic light scattering (DLS) measurement (Fig. 1(A)). The average PDI was estimated to be 0.133 ± 0.01 and 0.166 ± 0.022, respectively. CSNPs (36 ± 2 mV) and Mel-CSNPs (35 ± 1 mV) showed positive zeta potential attributed to cationic nature of Chitosan (Fig. 1 (B)). We observed a slight reduction in zeta potential in Mel-CSNPs which may be due to loading of melatonin. As nanoparticles were intended for intravenous (i.v.) administration controlling size is an important aspect which was observed through TEM images. Hence,

Journal of Chemical Health Risks

www.jchr.org

JCHR (2024) 14(6), 2129-2143 | ISSN:2251-6727

surface morphology images obtained through TEM confirmed the spherical and monodisperse nature of our formulations (Fig. 1 (C)). FESEM images also confirm the spherical and monodisperse nature of nanoparticles (Fig. S1). Results of morphological and size analysis is lieu to the earlier reports that has shown spherical shape of melatonin loaded chitosan nanoparticles with size of 110–300 nm range [27].

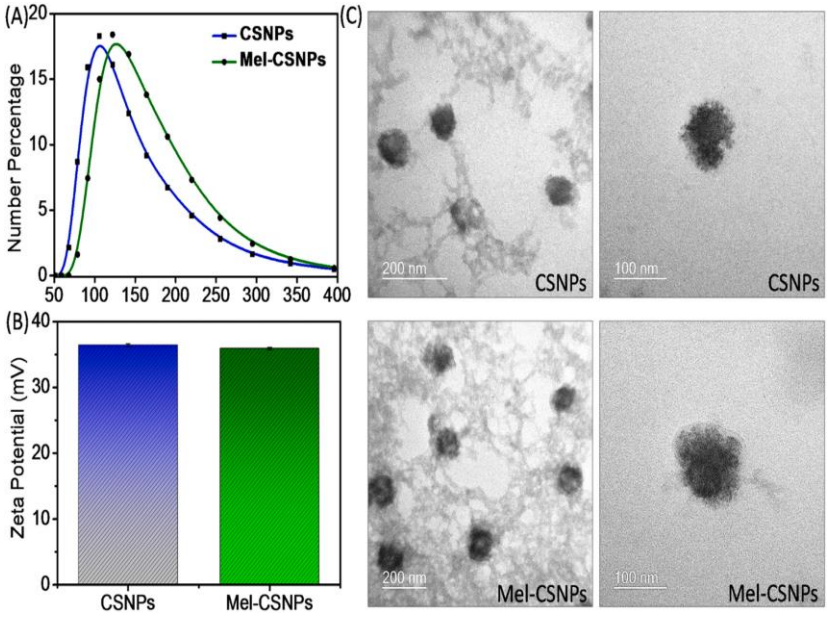

Fig. 1. Characterisation of nanoparticles (A) Dynamic Light scattering measurement of mean hydrodynamic size of chitosan nanoparticles (CSNPs) and Melatonin loaded chitosan nanoparticles (Mel-CSNPs) (B)-Surface zeta potential measurement of CSNPs (+ 36 ± 2 mV) and Mel-CSNPs (+35 ± 1 mV) and (C)TEM images of CSNPs and Mel-CSNPS shows nano-sized particles.

Fourier transform infrared spectroscopy (FT-IR) and X-ray diffraction (XRD) analysis

Chitosan showed a major hydroxyl (-OH) absorption band obtained 3400 cm- 1 and free amino (- NH2) at C2 position in glucosamine 1157 cm- 1 peak obtained denotes -C-O-C-bridge that confirms chitosan presence [28]. C-O stretching of primary alcohol peak at 1379 cm- 1 was observed in Chitosan. Melatonin showed a sharp peak at 3300 cm- 1 for N–H bending and a peak at 3078 cm- 1 for C–N stretching. Melatonin peaks 1495 cm- 1 and 1556 cm- 1 for aromatic -C = and 1627 cm- 1 for -C=O. CSNPs showed broadened -OH stretching peak at 3400 cm- 1 which may be attribute due to formation of nanoparticle and difference between Mel-CSNPs and CSNPs spectrum, FTIR indicates complete encapsulation of melatonin (Fig. S2(A)). X-ray Diffraction (XRD) study was done for evaluation of physical nature of chitosan, melatonin, CSNPs and Mel-CSNPs. Chitosan showed broad diffractions peaks at 10.43◦ and 20.31◦ which indicates its low degree of crystalline nature that is in agreement of previous study. Melatonin showed highly sharp and intense peak at 10.75◦, 11.42◦, 14.76◦, 16.45◦, 18.89◦, 20.48◦, 22.53◦, 24.14◦ and 24.93◦ indicating highly crystalline nature of melatonin [29]. CSNPs has shown more broad diffraction peak at 20.31◦ and Mel-CSNPs also shown similar diffraction pattern with minute crystalline peaks of melatonin that confirms presence of melatonin in chitosan nanocarrier [30]. The results are in support of existing literature that shown XRD analysis of chitosan nanoparticles and melatonin loaded chitosan nanoparticles that indicate amorphous structure of nanoparticles [31] (Fig. S2 (B)). Further, drug loading efficiency of our nanoformulation was obtained at different drug polymer weight ratio 1:10 (3.1%), 1:5 (8.5%) and 1:2 (20.4%). We have used the optimum drug loading at ratio 1:2 which is 20.4% for our study. The synthesized nanoformulation has shown better loading efficiency (20.4%) than existing report of melatonin loaded lecithin/chitosan nanoparticles (7.2%)

Journal of Chemical Health Risks

www.jchr.org

JCHR (2024) 14(6), 2129-2143 | ISSN:2251-6727

that indicates better property of our nanoformulation [32].

In-vitro drug release study

The drug release profile from Mel-CSNP showed a biphasic pattern *i. e.* initial burst release followed by prolonged release. Initially, within 1 h of experiment Mel-CSNP showed cumulative release of 22.05% and by the end of 24 h, it is up to 76.35% cumulative release in PBS pH 7.4. Biphasic drug release from nanoparticles is one of major reason for improving therapeutic efficacy of melatonin which has poor retention time in body that in agreement with previous study. (Fig. 2 (A)). Drug release study in acidic condition at pH 4.5 showed similar pattern as in PBS pH 7.4 but was faster and more release of drug occurred at 24 h which is up to 96.22% (Fig. S3).

In-vitro cellular internalization of nanoparticles

FITC-tagged Mel-CSNP showed higher accumulated cytoplasmic uptake 1 h post treatment (Fig. 2 (D)). This indicates the potential of nanoparticles to permeate cells to deliver drugs. Here, RAW 264.7 murine macrophages which has basic physiological role of phagocytosis which could be considered as possible mechanism of the cellular internalization of nanoparticle.

In-vitro anti-inflammation analysis

Chitosan is a highly biocompatible and non-toxic polymer. Hence, CSNPs and Mel-CSNPs did not show any significant cytotoxicity. In Fig. 2 (B) CSNPs and Mel-CSNPs used at various concentrations up to 1000 µg/mL did not show any significant cytotoxicity which is in lieu to reports that demonstrated highly biocompatible nature of CSNPs [33]. In order to estimate anti-inflammatory potential of melatonin and Mel-CSNP, RAW 264.7 cells were stimulated with lipopolysaccharide (LPS) to generate inflammatory response. LPS has the ability to generate inflammatory immune response by stimulating TLR-4 receptors. 1 µg/mL dose of LPS, a bacterial endotoxin has been utilized by following existing reports to induce inflammation. The results have shown anti-inflammatory action of Mel-CSNPs and melatonin, both (Fig. 2(C)) by reducing 55% and 40% NO generation. Herein, we found superior protective efficiency of our nanoformulations in comparison to existing report of melatonin that has shown 10% nitrite reduction at 250µM dose. In addition, they have demonstrated a higher 60% reduction with 2000 µM dose. Indeed, our nanoformulation has shown 55% NO reduction at 200 µM dose of melatonin. It indicates improved melatonin anti-inflammatory efficiency due to chitosan nano formulation. It further benefits to reduce the required effective drug concentration in the treatment of inflammatory diseases [34].

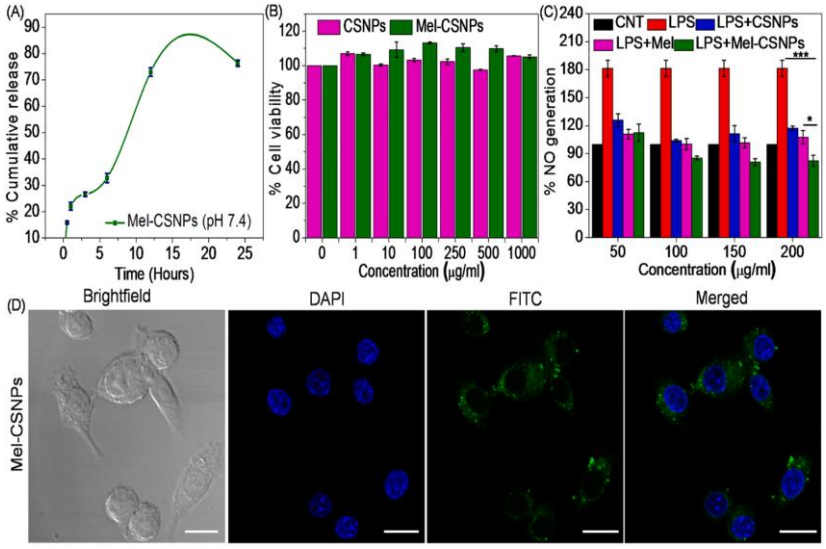

Fig. 2. (A) *In-vitro* drug release indicates biphasic release, (B) MTT assay for biocompatibility of nanoformulation, (C) Nitrite estimation for anti-inflammatory activity assessment,(D) Confocal laser microscopy (CLSM) images show major cytoplasmic accumulation of nanoparticles.(*$p \leq 0.05$, **$p \leq 0.001$ and ***$p \leq 0.0001$)(Scale bar = 20 µm).

Journal of Chemical Health Risks

www.jchr.org

JCHR (2024) 14(6), 2129-2143 | ISSN:2251-6727

Nuclear factor kappa-light-chain-enhancer of activated B (NF-κB) p65 - nuclear translocation study

NF-κB p65 is a family of inducible transcription factors, which regulates a variety of genes involved in various processes of the immune and inflammatory responses. LPS binds to TLR4 receptors of macrophages and activates the translocation of NF-κB p65 transcription factor from cytoplasm into the nucleus, which triggers the transcription of target genes [35, 36]. In Fig. 3,pre-treatment of Mel-CSNP (200 µg/mL) showed better anti-inflammatory response by interfering with the nuclear translocation of NF-κB p65 compared to bare melatonin and placebo CSNPs treatment group. Inhibition of NF-κB p65 nuclear translocation by our nanoformulation indicates its anti-inflammatory action. These results are in lieu to reports that have demonstrated inhibition of NF-κB p65 nuclear translocation as effective therapeutic potential of anti-inflammatory agents [37]. Immunofluorescence studies with LPS (1 µg/mL) activated RAW264.7 macrophage cell line showed active nuclear translocation in comparison to the only LPS treated cells. Hence, Mel-CSNPs attenuate gene expression of various NF-κB p65 target inflammatory genes which exacerbates inflammatory response. Agreement for results of MTT assay, NO estimation and NF-κB p65 nuclear translocation confirms anti-inflammatory action and therapeutic potential of our nanoformulations [38].

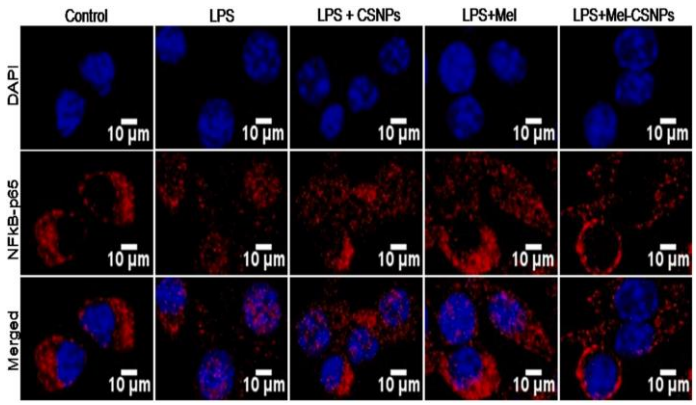

Fig. 3. CLSM micrographs reflect anti-inflammatory action of Mel-CSNPs by showing reduction in nuclear translocation of NF-κB p65 against LPS stimulation.

Haemolysis analysis

The haemolysis test was performed to analyse haemocompatibility of nanoparticles for its safe application through intravenous route. The results of the haemolysis test have shown no significant difference for Mel-CSNPs and CSNPs at doses of 1 mg/mL and 5 mg/mL, respectively (Fig. S4).This suggests our nanoformulation is safe for intravenous application and does not cause lysis of red blood cells. The results are in well accordance to the report that has demonstrated better heamocompatibility of chitosan nanoparticle. Intravenous administration of chitosan nanoparticles has shown specific targeting due to their nature [39].

***In-vivo* biodistribution study**

In-vivo biodistribution study of ICG-tagged Mel-CSNP showed initial distribution in highly perfused tissue *i.e.* heart and liver as shown in Fig. 4. The reduction in fluorescence intensity was seen during later time points indicating gradual clearance of nanoparticles from the body [40]. As a result the fluorescence intensity in the kidney and liver was increased compared to the initial time point that indicates clearance path of nanoparticles. Results are in lieu to existing reports that indicate liver and kidney mediated clearance path of nanoparticles [41]. Also, *ex-vivo* imaging showed that there was lower fluorescence intensity in vital organs like brain, kidney liver, heart and spleen due to low retention and clearance of nanoparticles from these organs. However, high fluorescence intensity observed in target colonic tissue shows higher retention of nanoparticles in colon. This is might be due to higher availability and expression of melatonin receptors and higher accumulated proportion of macrophages in colonic region [42, 43].

Journal of Chemical Health Risks

www.jchr.org

JCHR (2024) 14(6), 2129-2143 | ISSN:2251-6727

***I*n-vivo therapeutic efficacy study**

In order to assess the therapeutic efficacy of nano-formulation, the Disease Activity Index was calculated for each experiment to understand severity of disease caused due DSS treatment. The desired therapeutic effect of melatonin and Mel-CSNPs was also monitored in DSS induced ulcerative colitis in mice. The higher DAI suggests severe inflammatory pathological conditions like diarrhoea and bleeding in DSS induced colitis mice and significant recovery has been observed with Mel-CSNPs in comparison of other treatment groups (Fig. 5(A)). As shown in Fig. 5(A) there was no significant difference observed in melatonin and Mel-CSNPs groups but after 5th day onwards Mel-CSNPs exhibited significant improvement in therapeutic efficacy compared to bare melatonin. Similarly, in Fig. 5(B), the significant restoration of body weight has been noted with MelCSNPs treatment in comparison to melatonin treatment group against DSS induced weight loss. Leaky gut pathological conditions causeweight loss due to compromised gut function which arises due to DSS challenge in mice. Indeed, the recuperative effect of Mel-CSNPs has been confirmed by observing negligible reduction in colon length with respect to control

group versus DSS induced colon damage in Fig. 5(C–D). Herein, our Mel CSNPs has shown better *in-vivo* therapeutic efficacy in comparison to bare melatonin in terms of colon length parameter analysis. Hence, our nanoformulation has exhibited its therapeutic efficiency by improving health measures of mice having DSS induced IBD symptoms. Bare melatonin having short plasma half-life in the body is cleared out of the system which may be the possible cause of compromised antiinflammatory activity [44]. Mel-CSNPs exhibited significant improvement in anti-inflammatory activity which is apparent from results depicted in Fig. 5.

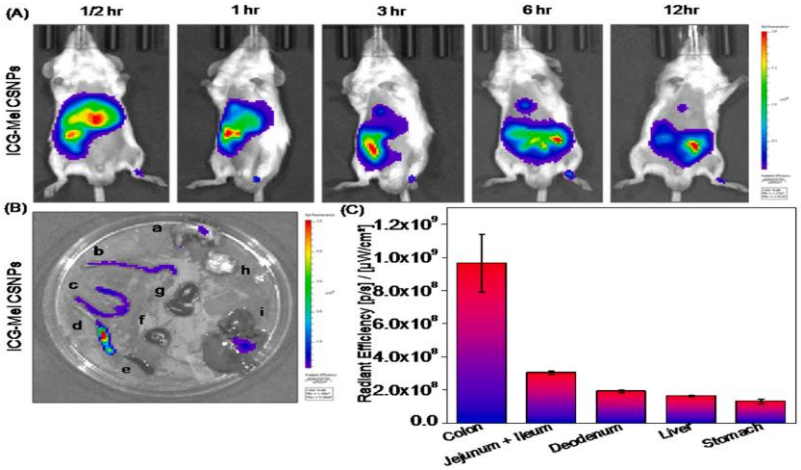

Fig. 4. (A) *In-vivo* bio-distribution study of Indocyanine green (ICG)-tagged Mel-CSNPs and (B–C)–*Ex-vivo* bio-distribution of ICG-Mel-CSNPs, (a- stomach, bdeodenum, c- ileum+jejunum, d- colon, e- spleen, f- heart, g- kidney, h- brain and i- liver) show good bio-distribution and clearance path of nanoparticles. (For interpretation of the references to colour in this figure legend, the reader is referred to the web version of this article.)

Journal of Chemical Health Risks

www.jchr.org

JCHR (2024) 14(6), 2129-2143 | ISSN:2251-6727

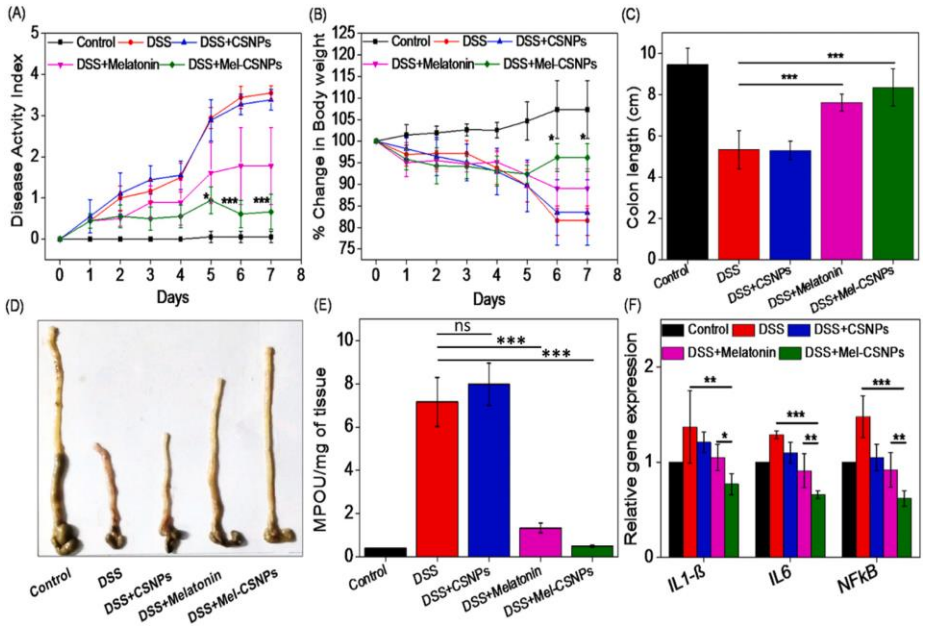

Fig. 5. (A)- Disease Activity Index, (B) Percentage change in body weight,(C–D) Colon length evaluation, (E) Myeloperoxidase (MPO) assay in colonic tissue homogenates and(*F*)Gene expression of analysis in colonic tissue sample of mice confirms anti-inflammatory potential of Mel-CSNPs.(*$p \leq 0.05$, **$p \leq 0.001$, ***$p \leq 0.0001$and ns: non-significant).

Myeloperoxidase assay

Myeloperoxidase (MPO) activity is linked with degree of intestinal inflammation and neutrophilic infiltration. Higher number of neutrophilic infiltration is observed during inflammatory condition [45]. MPO is present in neutrophil which can be used to assess degree of neutrophilic infiltration and inflammation. The efficiency to prevent infiltration of immune cells to the disease sites proves the anti-inflammatory potential of therapeutic agent. In correspondence of it, MPO activity is found higher in group 2: DSS and group 3: DSS + CSNPs, whereas it was significantly reduced in group 4: DSS + Melatonin and group 5: DSS + Mel-CSNPs in Fig. 5(E).This results shows superior anti-inflammatory efficiency of our nanoformulation in comparison to existing report of anti-inflammatory agents by reducing double fold infiltration of immune cells to DSS induced colon [46]. Here, Mel-CSNPs has exhibited more reduction in MPO activity in comparison to bare melatonin that indicates improvement in therapeutic efficiency by nanotherapeutic approach. Thus, results of MPO activity have revealed anti-inflammatory activity of our nanoformulation. The gene expression analysis of inflammatory genes has been performed to confirm this claim [47].

qPCR analysis – gene expression study

In DSS induced mice model of Ulcerative colitis there was significant up regulation gene expression of various inflammatory genes like IL-1β, IL-6 and NF-κB [48]. Hence, we have analysed expression of IL-1B, IL-6 and NF-κB to confirm anti-inflammatory action of our nanoformulation. In results, the significant reduced expression of inflammatory genes was found with treatment of our nanoformulation against DSS induced insults in Fig. 5(F). The results have shown similar double fold decreases compare to the reports that have shown reduction in inflammatory markers as therapeutic activity of anti-inflammatory agents [49]. There is one fold down regulation of inflammatory markers with Mel-CSNPs in compare to Melatonin against DSS induced expression reflects improvement in therapeutic activity due to nanoformulation in compare to bare melatonin [50].

Haematoxylin and eosin staining

Histopathological examination was done using Haematoxylin and Eosin (H&E) staining on colonic

Journal of Chemical Health Risks

www.jchr.org

JCHR (2024) 14(6), 2129-2143 | ISSN:2251-6727

tissue sections to analyse protection against DSS induced toxicological demarcation. As shown in Fig. 6(A), microscopic images of colonic tissue sections of different treatment groups were stained with H&E. Control group showed normal colonic tissue morphology whereas the DSS treated group showed complete damage of colonic crypt and villi. Higher amount of immune cell infiltration in colonic tissue sections of DSS treated groups has been observed. The DSS + CSNPs exposed group has not shown reduction in immune cell infiltration which is shown in Fig. 6(A) indicates a significant difference when compared between bare Melatonin and Mel-CSNPs treated group. Also, the results are in agreement of results of MPO activity that confirms nanoformulation improved anti-inflammatory action in respect to bare Melatonin in treatment of DSS induced IBD. Mel-CSNPs exhibited improvement in anti-inflammatory therapeutic efficacy of melatonin which is obvious from the gross pathological *in-vivo* therapeutic evaluation depicted in Fig. 5. Further these results were more strongly supported and proved by histological evaluation performing H&E study. Histopathological analysis revealed remarkable inflammatory pathological changes in a cross section of colon, like epithelial layer erosion, fibrotic changes, immune cell infiltration, goblet cell damage *etc.*, which was significantly attenuated in Mel-CSNPs suggesting its therapeutic efficacy.

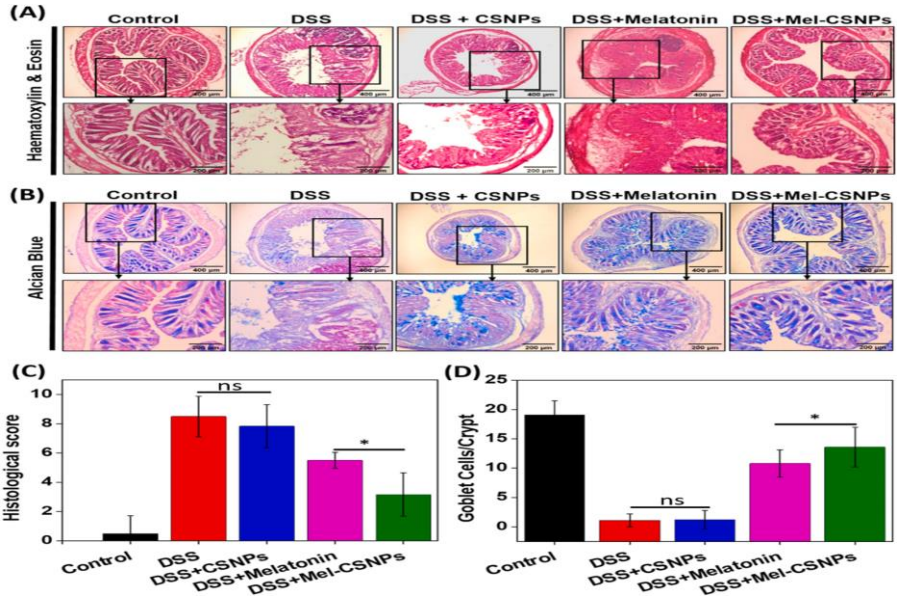

Fig. 6. A- Haematoxylin and Eosin (H&E) staining of cross section of colon (7 µm) indicates pathological demarcation. B- Alcian Blue and Nuclear Fast Red (AB-NR) staining of cross section of colon (7 µm)for evaluating goblet cells (Blue) and epithelial cells (Red) (C) Histological score for H&E stained cross section of colon. (D)

Goblet cell(s) count per crypt in the cross section of colon. (*$p \leq 0.05$, **$p \leq 0.001$, ***$p \leq 0.0001$and ns: non-significant).

Alcian blue and nuclear fast red staining

Alcian blue staining was done to evaluate loss of goblet cell number and damage occurred during DSS-induced inflammatory conditions in the mouse. In Fig. 6(B) the control group showed normal goblet cells number in crypt of colonic tissue sections. In colonic tissue sections of DSS and DSS + CSNPs treatment groups there is a remarkable decrease in goblets cell number per crypt which indicates the extent of severity and damage occurred during inflammatory conditions. Crypt destruction occurs due DSS induced epithelial damage in mice results in depletion of goblet cells which are responsible for maintaining the gut homeostasis and protect the epithelial layer against pathogenic insults by secreting mucin a sticky protective substance. While DSS + MelCSNPs has exhibited better prevention in immune cell infiltration and negligible damage to the colonic crypt in comparison to DSS + Melatonin treated group. There was a significant amount of goblet cells found in

Journal of Chemical Health Risks

www.jchr.org

JCHR (2024) 14(6), 2129-2143 | ISSN:2251-6727

colonic tissue sections of DSS + Melatonin (10.8 goblet cell/ crypt) and DSS + MelCSNP groups (13.6 goblet cell/ crypt). This result also reflects better therapeutic efficiency of Mel-CSNPs in comparison to bare melatonin. Our study suggests that bare melatonin and Mel-CSNPs showed protection against DSS induced epithelial damage leading to goblet cells depletion and crypt damage which is in line with earlier studies Moreover, the present study adds that nanoformulations of melatonin improves the therapeutic potential significantly which is shown in Fig. 6 (C) and (D) [51].

Nitric oxide synthase 2 (NOS2) and nitro-*tyrosine*

Immuno-histochemical (IHC) analysis has been performed to confirm the mechanism of nanoformulation as an anti-inflammatory agent. In result, IHC analysis has shown upregulation of inflammatory biomarkers like NOS2 and Nitro-tyrosine in DSS induced inflammation in mice as shown in Fig. 7(A). Nitric oxide synthase (NOS2) is an inflammatory biomarker, with elevated infiltrated inflammatory M1 macrophages in DSS induced colitis condition. In contrast, DSS + Mel-CSNPs treated group has shown remarkable down regulation in NOS2 expression in comparison to bare Melatonin treated group as shown in Fig. 7(A). The fluorescence intensity is quantified and is found to significantly reduced in Fig. 7(B) of DSS+ Mel-CSNPs treated compared to bare DSS + Melatonin treated group which suggests improvement in therapeutic potential of nanoformulations. Melatonin is known to reduce NOS2 expression in murine ulcerative colitis models. Here, we have explored the improvement in anti-inflammatory activity of melatonin loaded nanoformualtion which results improved therapeutic efficacy of melatonin. Melatonin can also act by down regulating innate immune system in order to modify host response leading to reduction in inflammatory process. Macrophages are essential part of innate immune response; hence melatonin causes reduction in macrophage expression resulting in its anti-inflammatory activity. Inhibition of NOS2 by melatonin is linked with its effect on NF-κB expression [52]. In this study we have investigated nuclear translocation of NF-κB p65 which is inhibited by melatonin and melatonin loaded nanoformulations which results in reduced expression NOS2 in colonic tissue. Melatonin loaded nanoformulation demonstrated significant reduction in NOS2 expression which resulted in improved therapeutic efficacy. The increased expression of NOS2 results in increased production nitrite radical which assists in formation of increased oxidative stress. These results in increased level oxidative stress which causes uncontrolled inflammation and thereby resulting pathological damage to colonic tissue. in mice as shown in histopathological examination study in Fig. 6 where H&E staining performed on DSS challenged mice results in increased pathological score compared to control where no damage is observed. Melatonin and Mel-CSNPs significantly improved pathological score even when challenged with DSS. Similarly, immuno-histochemical analysis of Nitro-tyrosine was performed to evaluate degree of peroxynitrite mediated protein nitrosylation occurred during DSS induced colitis in mice. Nitro-tyrosine expression was highly upregulated in DSS induced colitis mice [53]. In biological system tyrosine nitration occurs as part of oxidative damage or stress that results from pathological condition. In Fig. 8(A), higher reduction in fluorescence intensity of nitrotyrosine expression confirms better therapeutic efficacy of our nanoformulations in compare to bare Melatonin by reversing the DSS induced pathogenic signatures [54]. As shown in Fig. 8(B) quantification of fluorescence intensity is evaluated for comparative study of efficacy of bare Melatonin treated group and nanoformulations treated group which clearly suggests significant reduction in expression of nitrosylation status in colonic tissue cross section resulting in improvement in therapeutic efficacy of Melatonin. Our results are in compliance with earlier studies performed using melatonin against inflammatory pathological condition. Overall, Mel-CSNPs have proved its immense anti-inflammatory and therapeutic potential with support of the various results of *in-vivo* therapeutic assessments. The better therapeutic efficacy than bare melatonin proves that Mel-CSNPs endow anti-inflammatory activity in prevention of IBD [55].

Journal of Chemical Health Risks

www.jchr.org

JCHR (2024) 14(6), 2129-2143 | ISSN:2251-6727

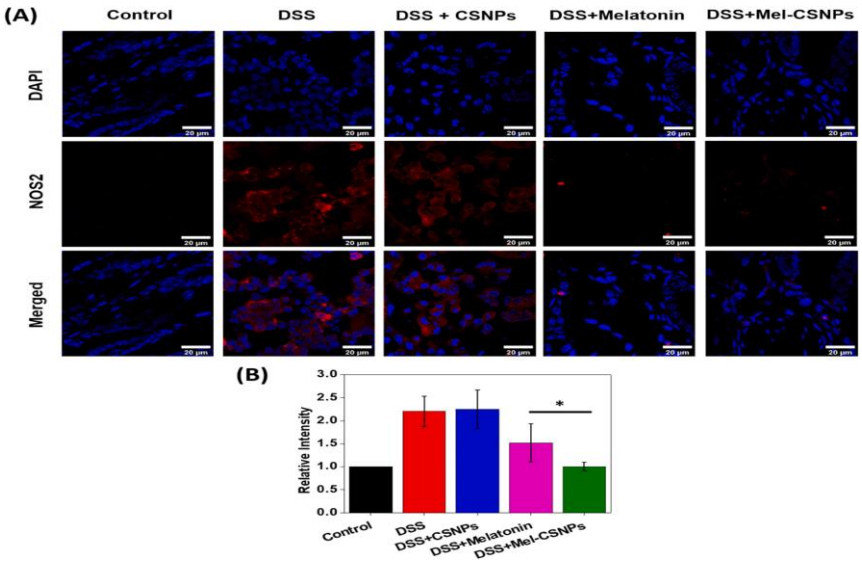

Fig. 7. (A) Immuno-histochemical staining of Nitric Oxide synthase 2 (NOS2) indicates M1 macrophage infiltration due to inflammation (B) Quantification of the fluorescence intensity. (*$p \leq 0.05$, **$p \leq 0.001$ and ***$p \leq 0.0001$).

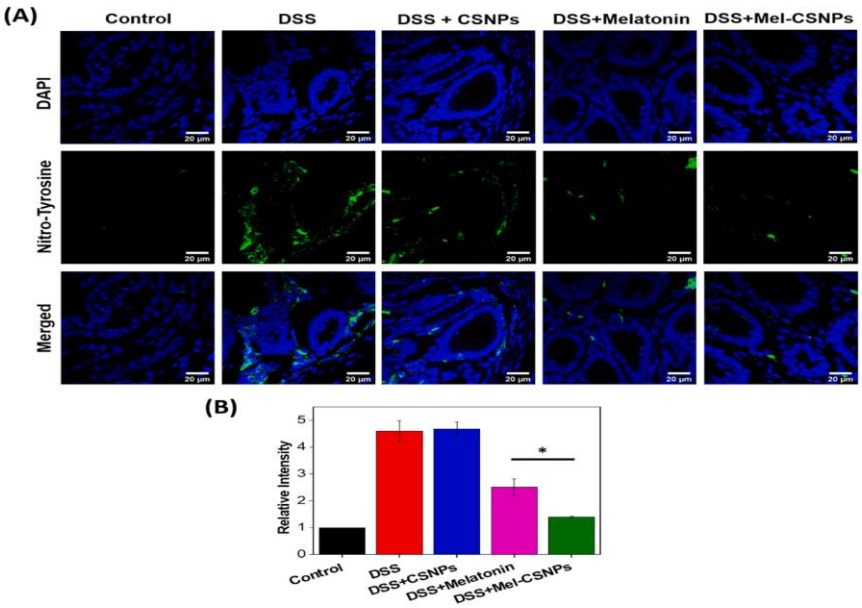

Fig. 8. (A) Immuno-histochemical stained CLSM images for Nitro-tyrosine represents inflammatory condition (B) Quantification of the fluorescence intensity. (*p ≤ 0.05, **p ≤ 0.001 and ***p ≤ 0.0001).

4. Conclusions

The results of study indicate that Mel-CSNPs significantly improves anti-inflammatory activity both *in-vitro* and *in-vivo* in comparison to bare melatonin. The reduction of NF-κB p65 nuclear translocation and nitric oxide reduction confirms anti-inflammatory potential of Mel-CSNPs against *in-vitro* LPS induced IBD models. Remarkable decrease in disease activity index (DAI) and Myeloperoxidase (MPO) activity proves *invivo* therapeutic efficiency of our nanoformulation by reducing infiltration of immune cells to disease sites. The down regulation of IL-1ß, IL-6, NF-κB gene markers and NOS2, Nitro-tyrosine inflammatory signature molecules divulge immense anti-inflammatory activity of our nanoformulation. Thus, the comprehensive analysis of the *in-vitro* and *in-vivo* study provides strong evidence toward

Journal of Chemical Health Risks

www.jchr.org

JCHR (2024) 14(6), 2129-2143 | ISSN:2251-6727

improvement of antiinflammatory activity with use of nanotherapeutic strategy compared to bare melatonin in IBD treatment.

Declaration of competing interest

The authors declare no conflict of interest, financial or otherwise.

Acknowledgements

This research did not receive any specific grant from funding agencies in the public, commercial, or not-for profit sectors. The authors are helpful to the National Institute of Technology (NIT), Rourkela, Odisha, India for providing all required facilities.

References

[1] R.J. Xavier, D.K. Podolsky, Nature 448 (2007) 427–434.

[2] D.C. Baumgart, W.J. Sandborn, Lancet 369 (2007) 1641–1657.

[3] B.A. Hendrickson, R. Gokhale, J.H. Cho, Clin. Microbiol. Rev. 15 (2002) 79.

[4] P.D. Castro, G. Harkin, M. Hussey, B. Christopher, C. Kiat, J.L. Chin, V. Trimble, D. McNamara, P. MacMathuna, B. Egan, B. Ryan, D. Kevans, M. Abuzakouk, R. Farrell, C. Feighery, V. Byrnes, N. Mahmud, R. McManus, United European Gastroenterol J 8 (2020) 148–156.

[5] G.B.D.I.B.D. Collaborators, Lancet Gastroenterol. Hepatol. 5 (2020) 17–30.

[6] M.A. Raad, N.H. Chams, A.I. Sharara, Inflamm. Intest. Dis. 1 (2016) 85–95.

[7] A. Kumar, M. Auron, A. Aneja, F. Mohr, A. Jain, B. Shen, Mayo Clin. Proc. 86 (2011) 748–757.

[8] G. Negi, A. Kumar, S.S. Sharma, J. Pineal Res. 50 (2011) 124–131.

[9] G. Negi, A. Kumar, R.K. Kaundal, A. Gulati, S.S. Sharma, Neuropharmacology 58 (2010) 585–592.

[10] J.R. Friedman, J. Nunnari, Nature 505 (2014) 335–343.

[11] V. Dehousse, N. Garbacki, A. Colige, B. Evrard, Biomaterials 31 (2010) 1839–1849.

[12] U. Garg, S. Chauhan, U. Nagaich, N. Jain, Adv. Pharm. Bull. 9 (2019) 195–204.

[13] S. Kumar Yadav, A. Kumar Srivastava, A. Dev, B. Kaundal, S. Roy Choudhury, S. Karmakar, Nanotechnology 28 (2017), 365102.

[14] J.J. Kim, M.S. Shajib, M.M. Manocha, W.I. Khan, J Vis Exp, (2012) 3678.

[15] P. Calvo, C. Remunan-L ˜ opez, ´ J.L. Vila-Jato, M.J. Alonso, Pharm. Res., 14 (1997) 1431–1436.

[16] M. Sun, Z. Deng, F. Shi, Z. Zhou, C. Jiang, Z. Xu, X. Cui, W. Li, Y. Jing, B. Han, W. Zhang, S. Xia, Biomater. Sci. 8 (2020) 912–925.

[17] P. Calvo, C. Remunan-Lopez, J.L. Vila-Jato, M.J.J.o.A.P.S, Alonso 63 (1997) 125–132.

[18] L.Q. Jiang, T.Y. Wang, T.J. Webster, H.-J. Duan, J.Y. Qiu, Z.M. Zhao, X.X. Yin, C. L. Zheng, Int. J. Nanomedicine 12 (2017) 6383–6398.

[19] S. Mao, J. Chen, Z. Wei, H. Liu, D. Bi, Int. J. Pharm. 272 (2004) 37–43.

[20] J. Benevides Bahiense, F.M. Marques, M.M. Figueira, T.S. Vargas, T.P. Kondratyuk,

D.C. Endringer, R. Scherer, M. Fronza, Pharm. Biol. 55 (2017) 991–997.

[21] A.V. Bagaev, A.Y. Garaeva, E.S. Lebedeva, A.V. Pichugin, R.I. Ataullakhanov, F. I. Ataullakhanov, Sci. Rep. (2019) 4563.

[22] A. Dev, S.J. Mohanbhai, A.C. Kushwaha, A. Sood, M.N. Sardoiwala, S.R. Choudhury, S. Karmakar, Acta Biomater., 109 (2020) 121–131.

[23] L.A. Dieleman, A.S. Pena, ˜ S.G. Meuwissen, E.P. van Rees, Scand. J. Gastroenterol. Suppl., 223 (1997) 99–104.

[24] A.M. Abdelmegid, F.K. Abdo, F.E. Ahmed, A.A.A. Kattaia, Sci. Rep. 9 (2019) 10176.

[25] A. Arbab, G. Yocum, M. Rad, A. Khakoo, V. Fellowes, E. Read, J. Frank, NMR Biomed. 18 (2005) 553–559.

[26] X. Wang, X. Kong, Y. Qin, X. Zhu, W. Liu, J. Han, Food Funct. 10 (2019) 4608–4619.

Journal of Chemical Health Risks

www.jchr.org

JCHR (2024) 14(6), 2129-2143 | ISSN:2251-6727

[27] M. Shokrzadeh, N. Ghassemi-Barghi, Pharmacology 102 (2018) 74–80.

[28] M. Queiroz, K. Melo, D. Sabry, G. Sassaki, H. Rocha, Marine Drug 13 (2014) 141–158.

[29] B. Topal, D. Cetin Altindal, M. Gümüs¸derelioglu, ˘ Int. J. Pharm., 496 (2015).

[30] F. Noori Siahdasht, N. Farhadian, M. Karimi, L. Hafizi, RSC Adv. 10 (2020) 9462–9475.

[31] M. Ali, M. Aboelfadl, A. Seliem, H. Khalil, G. Elkady, Separation science and technology, (2018).

[32] A. Hafner, J. Lovri´c, I. Pepi´c, J. Filipovic-Grcic, J. Microencapsul., 28 (2011) 807–815.

[33] T. Joo, K. Sowndhararajan, S. Hong, J. Lee, S.-Y. Park, S. Kim, J.-W. Jhoo, Saudi J. Biol. Sci. 21 (2014) 427–435.

[34] C. Phiphatwatcharaded, A. Topark-Ngarm, P. Puthongking, P. Mahakunakorn, Drug Dev. Res. 75 (2014) 235–245.

[35] R. Moreno, J.-M. Sobotzik, C. Schultz, M.L. Schmitz, Nucleic Acids Res. 38 (2010) 6029–6044.

[36] O. Sharif, V.N. Bolshakov, S. Raines, P. Newham, N.D. Perkins, BMC Immunol. 8 (2007) 1.

[37] S. Ikeguchi, Y. Izumi, N. Kitamura, S. Kishino, J. Ogawa, A. Akaike, T. Kume, J. Pharmacol. Sci. 138 (2018).

[38] A. Grodzki, B. Poola, N. Pasupuleti, M. Nantz, P. Lein, F. Gorin, J. Pharmacol. Exp. Ther. 352 (2014).

[39] R. Nadesh, D. Narayanan, R.S. P, S. Vadakumpully, U. Mony, M. Koyakkutty, S. V. Nair, D. Menon, J. Biomed. Mater. Res. A 101 (2013) 2957–2966.

[40] M.N. Sardoiwala, A.K. Srivastava, B. Kaundal, S. Karmakar, S.R. Choudhury, Nanomedicine, 24 (2019) 102088.

[41] M.N. Sardoiwala, A.C. Kushwaha, A. Dev, N. Shrimali, P. Guchhait, S. Karmakar, S. Roy Choudhury, ACS Biomater. Sci. Eng., 6 (2020) 3139–3153.

[42] C.-Q. Chen, J. Fichna, M. Bashashati, Y.-Y. Li, M. Storr, World J. Gastroenterol. 17 (2011) 3888–3898.

[43] C.C. Bain, A, Schridde 9 (2018).

[44] V.G. Kokich, Am. J. Orthod. Dentofac. Orthop. 143 (2013) S11.

[45] J.E. Krawisz, P. Sharon, W.F. Stenson, Gastroenterology 87 (1984) 1344–1350.

[46] M. Davaatseren, J.-T. Hwang, J. Park, M.-S. Kim, S. Wang, M. Sung, Mediat. Inflamm., 2013 (2013) 982383.

[47] T. Bui Thanh, H. Thanh, H. Le Thi Thu, D. Huong, Merit Res. J. Med. Medical Sci. 2 (2014) 216–224.

[48] M. Per˘se, A. Cerar, J Biomed Biotechnol, 2012 (2012) 718617–718617.

[49] R.M. Gadaleta, K.J. van Erpecum, B. Oldenburg, E.C.L. Willemsen, W. Renooij,

S. Murzilli, L.W.J. Klomp, P.D. Siersema, M.E.I. Schipper, S. Danese, G. Penna, G. Laverny, L. Adorini, A. Moschetta, S.W.C.v, Mil, Gut 60 (2011) 463.

[50] J. D¨ abritz, L. Judd, H. Chalinor, T. Menheniott, A. Giraud, Sci. Rep. 6 (2016) 20584.

[51] S.W. Kim, S. Kim, M. Son, J.H. Cheon, Y.S. Park, Sci. Rep. 10 (2020) 2232.

[52] G. Kolios, V. Valatas, S.G. Ward, Immunology 113 (2004) 427–437.

[53] D.N. Seril, J. Liao, G.Y. Yang, Mol. Carcinog. 46 (2007) 341–353.

[54] J.S. Beckman, Chem. Res. Toxicol. 9 (1996) 836–844.

[55] S. Cuzzocrea, E. Mazzon, I. Serraino, V. Lepore, M.L. Terranova, A. Ciccolo, A. P. Caputi, J. Pineal Res. 30 (2001) 1–12.